Growth of Multilayer WSe_2/Bi_2O_2Se Heterostructures for Photodetection without Lithography

Jun-Cheol Park†[a], Seungkyu Kim[a], Hojoong Choi [a], Yoonsung Jung[a], Inhyeok Oh[a], Jun Beom Hwang[a], Sanghan Lee*[a]

[a] *School of Material Science and Engineering, Gwangju Institute of Science and Technology, Gwangju, 61005, Republic of Korea*

*Corresponding author: Sanghan Lee (sanghan@gist.ac.kr)

Preprint not peer reviewed

This preprint research paper has not been peer reviewed. Electronic copy available at: https://ssrn.com/abstract=4194617

Abstract

Novel oxychalcogenides, such as Bi_2O_2Se, have many applications because of their interesting properties such as remarkable hall mobility, presence of a bandgap, and high air stability. Among them, photodetectors based on Bi_2O_2Se are one of the best applicable devices. In addition, the Bi_2O_2Se heterostructure with other 2D materials can enhance the photoresponse of the device. In this study, we successfully fabricated the WSe_2/Bi_2O_2Se heterostructure for photodetector application via in situ pulsed laser deposition. The band alignment of the as-grown WSe_2/Bi_2O_2Se heterostructure was confirmed to be type II, which increases the photoresponse. Furthermore, the WSe_2/Bi_2O_2Se photodetector exhibited an approximately 110% on/off ratio with a photoresponsivity of 0.96 mA/W even without using lithography for its fabrication.

Preprint not peer reviewed

This preprint research paper has not been peer reviewed. Electronic copy available at: https://ssrn.com/abstract=4194617

Introduction

Two-dimensional (2D) materials such as layered metal chalcogenides (LMDs), graphene, black phosphorous (BP), and hexagonal boron nitride have drawn tremendous interest as promising materials for electronic and optoelectronic devices because of their extraordinary properties.[1–9] However, the practical applications of these conventional 2D materials for electronic and optoelectronic devices are limited because of the zero bandgap of graphene and air instability of LMDs and BP; therefore, the use of novel alternative 2D materials is required. Recently, Peng et al. reported the use of Bi_2O_2Se as a novel layered oxychalcogenide owing to its tremendous Hall mobility (~450 $cm^2 \cdot V^{-1} \cdot s^{-1}$ at RT and >20,000 $cm^2 \cdot V^{-1} \cdot s^{-1}$ at 1.9 K), non-zero bandgap (~1 eV), and high air stability.[10–15] Accordingly, Bi_2O_2Se was widely used for various applications such as field-effect transistors (FET), photodetectors, thermoelectrics, and memristors.[16–21] Among them, Bi_2O_2Se-based photodetectors are one of the most intensively studied applications because they show an ultra-fast photoresponse, high detectivity, and a wide photodetection range from visible to infrared.[14, 22–24] Despite many merits of Bi_2O_2Se and other 2D materials, there are some drawbacks, including the difficulty in synthesizing large-scale thin films, a non-sharp interface of heterostructures, and relatively complex device-fabrication processes when conventional synthesis methods such as hydrothermal, chemical vapor deposition, and mechanical exfoliation are used.[11, 25, 26]

Heterostructures with type-II band alignment have many advantages in terms of photoresponse. They can offer not only expansion of the response spectrum range by overcoming the intrinsic bandgap property but also high stability and low operation voltages.[27–31] Moreover, a type-II heterostructure facilitates separation of electron–hole pairs (EHPs), in turn enhancing the photoresponse of photodetectors.[32] In this perspective obstacles for photodetectors in Bi2O2Se which shows high dark current and relatively low on/off ratios could solve through type-II heterostructure.[33–35] Among the many candidates for 2D heterostructures with Bi_2O_2Se, we adopt WSe_2 for its desirable band position for the formation of type-II band alignment and strong light absorption, which consequently provides high photoconversion efficiency.[36, 37]

For high-performance photodetection, J. Sun et al. and X. Chen et al. reported the effect of piezo-phototronics in photodetection, overcoming the limitation of perovskite solar cell based photodetector and improving the transfer efficiency of the photon-generated carriers, respectively.[38, 39] Despite many efforts to enhance the performance of photodetection, direct and wafer-scale synthesis of heterostructure is challenged by limitation of methodologies. Recently, physical vapor deposition methods such as pulsed laser deposition (PLD) and molecular beam epitaxy have been reported for fabricating large-scale 2D materials.[40–42] Particularly, uniform and stoichiometric 2D chalcogenide thin films without deficiency of chalcogen atoms can be grown via PLD. Thus, it is suitable for the growth of large-scale 2D materials.[43] In addition, the number of layers, which affects various properties of 2D materials, can be precisely controlled via PLD.[44, 45] More interestingly, uniform 2D heterostructures without intermixing phases could be realized via direct in situ PLD.[46, 47] For these reasons, the PLD method is appropriate for manufacturing 2D heterostructures composed of Bi_2O_2Se, which is one of the ways of advancing the performance of photodetectors.

Usually, a complex lithography process, which involves patterning, lifting off, and deposition of electrodes, is essential for fabricating electronic devices. These processes leave a large amount of organic residue on the surface of thin films and at the interface between thin films and metals; this majorly affects the efficiency of the device. In particular, because conventional 2D materials such as transition-metal dichalcogenides (TMDs) are vulnerable to humidity, many studies have attempted to avoid a complex lithography process.[48–53]

This preprint research paper has not been peer reviewed. Electronic copy available at: https://ssrn.com/abstract=4194617

Herein, we present a simple process of device fabrication with the growth of centimeter-scale 2D WSe_2/Bi_2O_2Se thin films via PLD. First, we deposited multilayers of Bi_2O_2Se and WSe_2 on a c-plane Al_2O_3 substrate via direct in situ PLD (details in the experimental section). We further investigate the structural, electrical, and optical properties of the WSe_2/Bi_2O_2Se heterostructure grown by PLD. Finally, we fabricated WSe_2/Bi_2O_2Se photodetectors with a patterning-free process and investigated their optical characteristics.

Results and Discussion

To fabricate the in situ heterostructure of 2D materials (here, WSe_2/Bi_2O_2Se), we first deposited multilayers of Bi_2O_2Se and WSe_2 on a c-plane Al_2O_3 substrate through PLD (see the experimental section for the fabrication of Bi_2O_2Se and WSe_2 thin films). As previously reported, the PLD system can easily control the stacking order of thin films using a multi-carousel target rotation system as well as their thickness by adjusting the number of laser pulses.[45, 54] As shown in Figure 1a, all of the samples (WSe_2/Bi_2O_2Se heterostructures and single films of Bi_2O_2Se and WSe_2) were uniformly deposited on the c-plane Al_2O_3 substrate (10 mm × 10 mm) without any optical gradation. The thicknesses of the as-grown Bi_2O_2Se and WSe_2/Bi_2O_2Se heterostructures were 20 and 26 nm, respectively, as confirmed by atomic force microscopy (AFM) (Figure S1a and b). The schematic of Figure 1b illustrates the WSe_2/Bi_2O_2Se photodetectors fabricated using Cu wire and Ag paste without any additional patterning process.

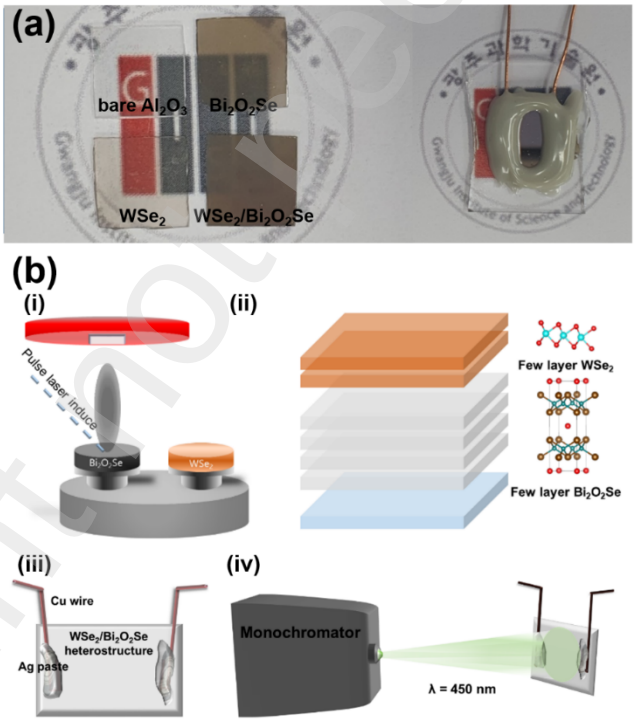

Figure 1. (a) Photograph of PLD-grown WSe_2/Bi_2O_2Se thin films on c-Al_2O_3. (b) Schematic of fabrication of the WSe_2/Bi_2O_2Se device, i) deposition of WSe_2/Bi_2O_2Se thin films via the PLD method, ii) stacking sequence of the heterostructure, iii) fabrication of the WSe_2/Bi_2O_2Se device with wiring, and iv) measurement of photoresponse using a monochromator with 450 nm wavelength.

This preprint research paper has not been peer reviewed. Electronic copy available at: https://ssrn.com/abstract=4194617

The structural properties of the WSe_2/Bi_2O_2Se heterostructures were further investigated by Raman spectroscopy in the range of 110–300 cm^{-1} for each sample. Figure 2a shows the results of Raman spectroscopy for Bi_2O_2Se (red line) and WSe_2/Bi_2O_2Se (blue line). As previously reported, a characteristic peak at 159 cm^{-1} (A_{1g}) caused by the out-of-plane vibrational mode of Bi_2O_2Se was clearly observed (Figure 2a).[55] Contrarily, in WSe_2/Bi_2O_2Se heterostructures, the overlapped peak ($E^1_{2g} + A_{1g}$) of WSe_2 (253 cm^{-1}) and peak of Bi_2O_2Se with a blue shift (169 cm^{-1}) were observed. Theoretically, the presence of a negative uniaxial strain, i.e., uniaxial compression, which occurs to modify the crystal phonons in low-dimensional materials cause a blue shift.[55] The known lattice constant of an axis of WSe_2 is defined as 3.286 Å, while that of an axis of Bi_2O_2Se is 3.88 Å. Therefore, lattice mismatch occurred during the in situ growth of WSe_2 and Bi_2O_2Se heterostructures. Consequently, the blue-shifted peak at 169 cm^{-1} for Bi_2O_2Se was caused by the negative uniaxial strain. For fabrication of large-scale 2D material-based electronic and optoelectronic devices, the spatial uniformity of thin films is one of the most important parameters. To confirm the uniformity of the WSe_2/Bi_2O_2Se heterostructure, we performed the Raman mapping measurements for the WSe_2/Bi_2O_2Se heterostructure (Figure 2b–d). First, the Raman spectra recorded at 11 different points of the heterostructure show clear peaks corresponding to WSe_2 (253 cm^{-1}) and Bi_2O_2Se (169 cm^{-1}). Although there was a slight difference in the peak intensity, we confirmed that all peaks corresponding to thin films were well matched. In addition, the Raman mapping of the WSe_2/Bi_2O_2Se heterostructure was obtained on the basis of peak intensities at the center of 169 and 253 cm^{-1}, which are the characteristic peaks of Bi_2O_2Se and WSe_2, as shown in Figure 2c and d, respectively. Although Raman mapping measurements were conducted under half of the area (5 mm × 5 mm) of the entire substrate (10 mm × 10 mm), the Raman spectra of Bi_2O_2Se and WSe_2 were clearly observed at the center position except for some points.

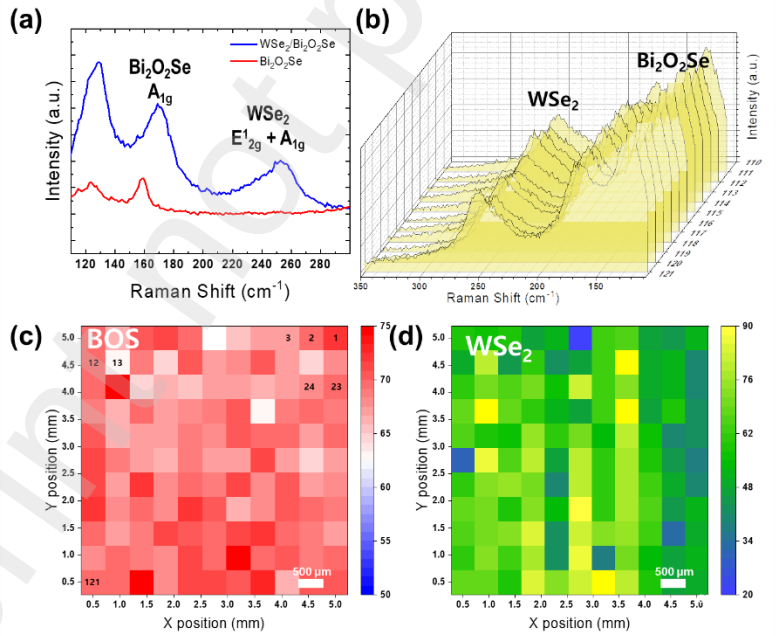

Figure 2. Structural analysis of WSe_2/Bi_2O_2Se. (a) Spectral acquisition of the Bi_2O_2Se single layer (red line) and the WSe_2/Bi_2O_2Se heterostructure (blue line). (b) Entire Raman spectra of the WSe_2/Bi_2O_2Se heterostructure from the last row (points 110 to 121). Raman mapping based on the peak intensity for (c) Bi_2O_2Se at 169 cm^{-1} and (d) WSe_2 at 253 cm^{-1} in the WSe_2/Bi_2O_2Se heterostructure.

This preprint research paper has not been peer reviewed. Electronic copy available at: https://ssrn.com/abstract=4194617

Furthermore, X-ray photoelectron spectroscopy (XPS) was performed to determine the chemical bonding characteristics of Bi_2O_2Se (Figure 3a–c) and WSe_2/Bi_2O_2Se (Figure 3d–g) thin films (XPS analysis of WSe_2 is shown in Figure S3). According to the Bi 4f spectra (Figure 3a), the two fitted peaks at 164 and 158.7 eV clearly matched the peaks of Bi $4f_{5/2}$ and Bi $4f_{7/2}$, which are attributed to Bi_2O_3 bonding. XPS spectra also showed the O 1s peaks at 530.9 and 529.6 eV caused by Bi_2O_3, as well as the doublet peaks corresponding to Se 3d at 53 and 53.8 eV. All of these binding energies of each spectrum could be assigned to the elements Bi, O, and Se of Bi_2O_2Se; this indicates that the chemical bonding characteristics of our Bi_2O_2Se thin film coincide with those reported in previous studies.[56] In addition, the XPS spectra show the peaks corresponding to each element, namely, Bi 4f, O 1s, W 4f, and Se 3d, for the WSe_2/Bi_2O_2Se heterostructure (Figure 3d–g); these are also consistent with those in previous reports.[36] However, there were some differences compared with the spectra of the single Bi_2O_2Se thin film. In addition to the peaks at 164 and 158.7 eV, the peaks in the XPS spectra of Bi 4f of the heterostructure were observed at 166 and 160.6 eV, which were due to the Bi_2Se_3 bonding. Likewise, the peak of O 1s also differed because of the hydroxyl group (–OH) and organic C–O bonding. As shown in Figure 3f, for W 4f of WSe_2, two major peaks and a relatively small peak can be ascribed to W^{4+} of $4f_{7/2}$ and $4f_{5/2}$ and W^{6+}, respectively, from oxidized W. As shown in Figure 3g, the spectra for Se 3d of the WSe_2/Bi_2O_2Se heterostructure have distinct peaks located at 55.3 and 54.5 eV caused by WSe_2 and 53.8 and 53 eV caused by Bi_2O_2Se. In addition, quantitative analysis indicates a Bi/Se ratio of 1.9:1 and a W/Se ratio of 1:2.2.

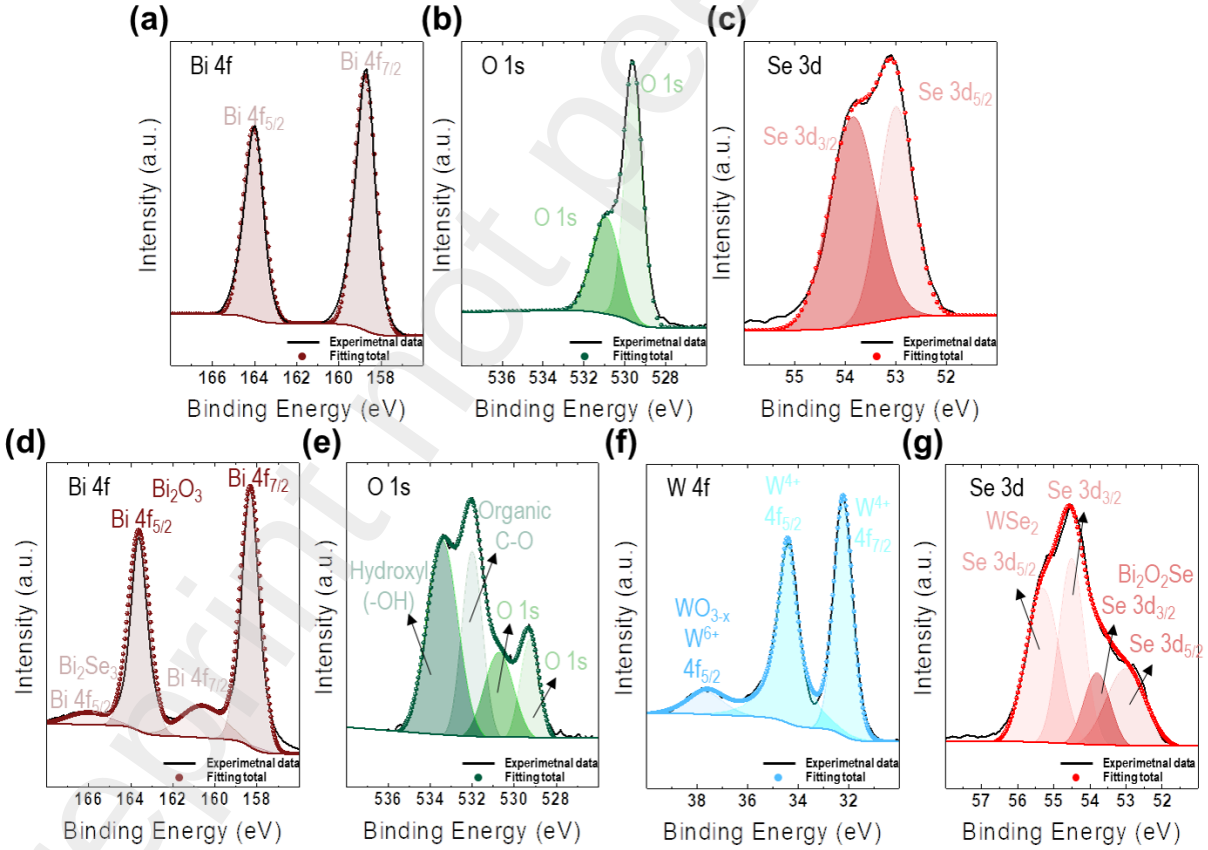

Figure 3. XPS spectra of (a) Bi 4f, (b) O 1s, and (c) Se 3d of the multilayers of Bi_2O_2Se. XPS spectra of (d) Bi 4f, (e) O 1s, (f) W 4f, and (g) Se 3d of multilayers of the WSe_2/Bi_2O_2Se heterostructure.

This preprint research paper has not been peer reviewed. Electronic copy available at: https://ssrn.com/abstract=4194617

The electronic structure and band gap of WSe_2 and Bi_2O_2Se thin films were investigated using ultraviolet photoelectron spectroscopy (UPS). As shown in Figure 4a and b, the work function (W) of each film was obtained on the basis of the difference in the photon energy (with He I light source, 21.21 eV) and the secondary electron cut-off energy. In addition, the valence band edges of the thin films were determined as 0.64 and 0.33 eV, respectively, by the lowest binding energy. Consequently, the formation of band alignment between WSe_2 and Bi_2O_2Se can be illustrated as the type-II heterojunction, as shown in Figure 4c. The band alignment of the WSe_2/Bi_2O_2Se heterostructure enables photogenerated carriers to be readily separated and transported to the electrodes, thereby improving the photoresponse compared to that of single-layer Bi_2O_2Se.

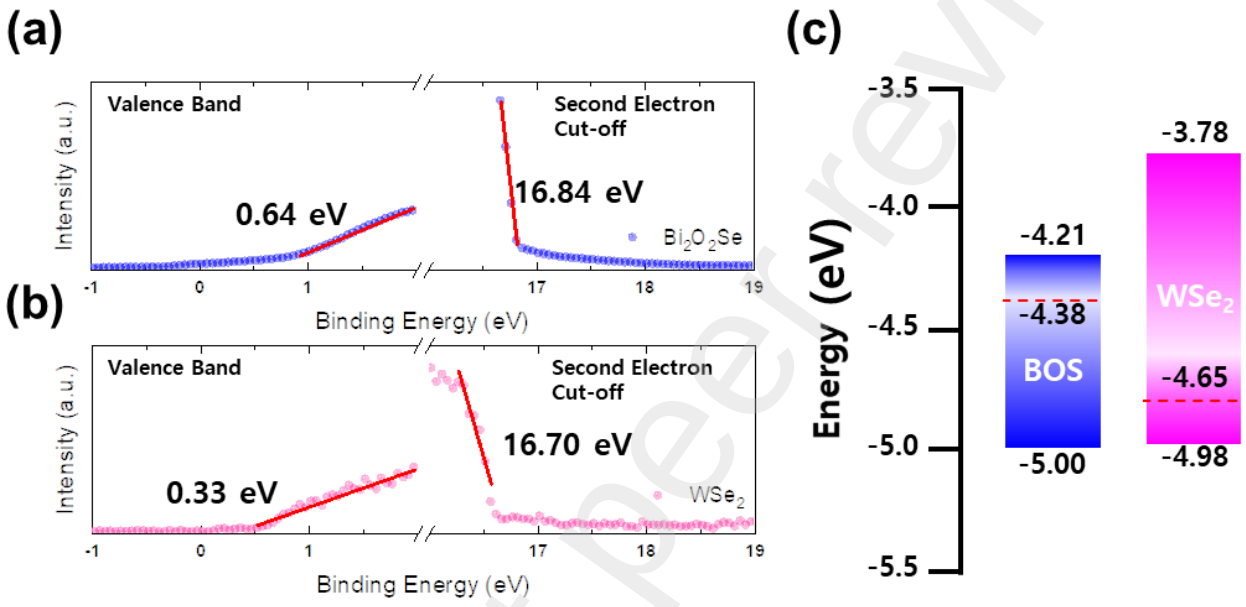

Figure 4. (a, b) UPS analysis for the electronic structure of Bi_2O_2Se and WSe_2, respectively. (c) Expected band alignment of the WSe_2/Bi_2O_2Se heterostructure.

After confirming the band alignment, we investigated the photoresponse characteristics of the WSe_2/Bi_2O_2Se heterostructure. Because Bi_2O_2Se shows extremely high mobility, photogenerated carriers from Bi_2O_2Se are expected to be readily separated.[32] The photoresponse characteristics of the WSe_2/Bi_2O_2Se heterostructure were evaluated with normalized time-dependent photoresponse under simulated chopped irradiation at an interval of 20 s of on and off with a repetition of 15 cycles. Consequently, we observed approximately 110% of on/off photoresponse ratio (Figure 5a). Compared to the WSe_2/Bi_2O_2Se heterostructure, multilayer Bi_2O_2Se thin films showed a lower photoresponse. The improved photoresponse characteristics of the WSe_2/Bi_2O_2Se heterostructure can be attributed to its type-II band alignment (Figure 4c), which induced the facile charge transfer of photogenerated carriers from the heterostructure. Responsivity, which is one of the most important factors in a photodetector, is defined as $R_{ph} = I_{ph}/(P_l \times A)$, where I_{ph} is the photocurrent, P_l is the incident light power, and A is the incident area. It was observed as 0.96 mA/W under a light intensity of 0.76 mW/cm^2 at 0.1 V. Considering that the wiring used in this study shows a relatively lower signal-to-noise ratio and higher ohmic drop compared to those of general electrode patterns such as interdigitated electrodes (IDEs), a 110% on/off ratio is a remarkable value.[57] Furthermore, as Figure 5b shows, the photocurrent of multilayer Bi_2O_2Se thin films exhibited extremely low on/off

This preprint research paper has not been peer reviewed. Electronic copy available at: https://ssrn.com/abstract=4194617

ratios; therefore, they are difficult to use as an optoelectronic device. This indicates that the type-II band alignment of the WSe_2/Bi_2O_2Se heterostructure is helpful in separating the photogenerated EHP. Figure 5c shows the enlarged range of the entire cycle. Rise (τ_r) and decay (τ_d) times are also defined as the time to transition between an increase of more than 90% from the minimum and a decrease of more than 90% from the maximum, respectively. As a result, the response time is τ_r = 0.5 s and τ_d = 1 s.

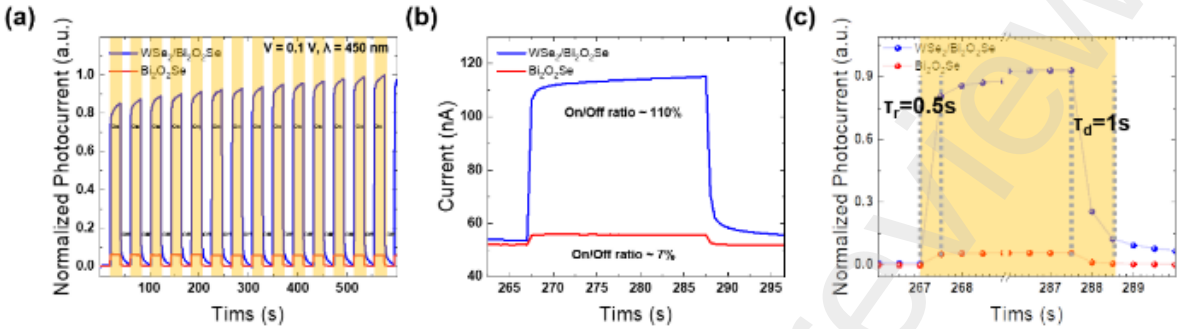

Figure 5. (a) Time-dependent normalized photoresponses of Bi_2O_2Se and WSe_2/Bi_2O_2Se heterostructures at 0.1 V under a wavelength of 450 nm. (red line: Bi_2O_2Se; blue line: WSe_2/Bi_2O_2Se). (b) Comparison of the on/off ratio. (c) The measurement of response speed of rise (0.5 and 0.5 s) and decay (1 and 0.5 s) times.

Conclusions

In summary, a centimeter-scale WSe_2/Bi_2O_2Se heterostructure-based optoelectronic device was successfully fabricated on an Al_2O_3 substrate by PLD. Structural and optical properties of the WSe_2/Bi_2O_2Se heterostructure were confirmed by AFM, Raman spectroscopy, and UPS, and high-quality-heterostructure thin films with type-II band alignment were confirmed. As a result, the photoresponse was evaluated as 0.96 mA/W. More interestingly, although the WSe_2/Bi_2O_2Se photodetector was fabricated without using lithography, it showed an on/off ratio of approximately 110% (the on/off ratio of the Bi_2O_2Se single film is only 7%). Thus, in this study, we improved the photoresponse by using the WSe_2/Bi_2O_2Se heterostructure while avoiding the complex device fabrication process of conventional 2D-material-based photodetectors.

Experimental Section

Growth of WSe_2/Bi_2O_2Se thin film: The Bi_2O_2Se and WSe_2 thin films were deposited on the Al_2O_3 substrate by PLD with a 248 nm KrF excimer laser (Coherent, Compex Pro 205F). We used supersaturated commercial targets (nonstoichiometric $WSe_{2.2}$ and a $Bi_2O_2Se_{1.3}$ target from LTS Research Laboratories) to prevent selenium deficiency. Acetone, methanol, isopropyl alcohol, and deionized water were used to remove organic particles and/or residues on the substrates. The Bi_2O_2Se layer was deposited at a 4 Hz repetition rate, a laser energy density of 1.8 $J \cdot cm^{-2}$, a substrate temperature of 400 °C, and a high vacuum condition (~2.0 × 10^{-6} Torr) without any carrier gas. Subsequently, WSe_2 was deposited at a 3 Hz repetition rate, a laser energy density of 1.1 $J \cdot cm^{-2}$, a substrate temperature of 400 °C, and a 100 mTorr Ar gas environment.

This preprint research paper has not been peer reviewed. Electronic copy available at: https://ssrn.com/abstract=4194617

Device fabrication: To determine the performance of WSe_2/Bi_2O_2Se heterostructure photodetectors fabricated without using a lithography process, we fabricated a two-terminal device by wiring with Cu wire and Ag paste. For the photoresponse test, a 150 W Xe lamp (Model 10500, ABET Technology) was used, which was calibrated as AM 1.5 G (100 $mW \cdot cm^{-2}$) using a Si photodiode (Bunkokeiki). The wavelength of the Xe lamp was controlled by a monochromator (Mmac 200, Dongwoo Optron).

Characterization of WSe_2/Bi_2O_2Se thin film: Raman spectroscopy (Renishaw, with wavelength of 514 nm) was used for structural analysis. Spectral acquisition was measured in the wavelength range of 110–300 cm^{-1}. To confirm the coverage of the heterostructure, Raman mapping was performed at 121 points in the range of 5 mm in width and height. The chemical state and electrical structure were confirmed by XPS and UPS (Thermo Fisher Scientific, Nexsa, monochromatic Al Kα line at 1486.69 eV based on C 1s at 284.8 eV).

Acknowledgments

This work was supported by a National Research Foundation of Korea (NRF) grant funded by the Korean government (MSIT) (Creative Materials Discovery Program-No.2017M3D1A1040834).

Keywords: Oxychalcogenide • bismuth oxyselenide • heterostructure • pulsed laser deposition • photodetection

[1] Z. Yin, ACS Nano, Single-Layer MoS_2 Phototransistors, 6 (2012) 74, DOI : 10.1021/nn2024557

[2] H. Wang, L. Yu, Y.-H. Lee, Y. Shi, A. Hsu, M. L. Chin, L.-J. Li, M. Dubey, J. Kong and T. Palacios, Integrated Circuits Based on Bilayer MoS_2 Transistors, Nano Lett. 12 (2012) 4674-4680, DOI : 10.1021/nl302015v

[3] L. Viti, J. Hu, D. Coquillat, W. Knap, A. Tredicucci, A. Politano and M. S. Vitiello, Black Phosphorus Terahertz Photodetectors, Adv. Mater. 27 (2015) 5567-5572, DOI : 10.1002/adma.201502052

[4] R. A. Street, Thin-Film Transistors, Adv. Mater. 21 (2009) 2007, DOI : 10.1002/adma.200803211

[5] A. Splendiani, Emerging Photoluminescence in Monolayer MoS_2, Nano Lett. 10 (2010) 1271, DOI : 10.1021/nl903868w

[6] F. Schwierz, Graphene transistors, Nat. Nanotechnol. 5 (2010) 487-496, DOI 10.1038/nnano.2010.89

[7] J. S. Ross, P. Klement, A. M. Jones, N. J. Ghimire, J. Yan, D. G. Mandrus, T. Taniguchi, K. Watanabe, K. Kitamura, W. Yao, D. H. Cobden and X. Xu, Electrically tunable excitonic light-emitting diodes based on monolayer WSe_2 p–n junctions, Nat. Nanotechnol. 9 (2014) 268-272, DOI : 10.1038/nnano.2014.26

[8] B. Radisavljevic, A. Radenovic, J. Brivio, V. Giacometti and A. Kis, Single-layer MoS_2 transistors, Nat. Nanotechnol. 6 (2011) 147, DOI : 10.1038/nnano.2010.279

[9] S. Helveg, Atomic-Scale Structure of Single-Layer MoS_2 Nanoclusters, Phys. Rev. Lett. 84 (2000) 951, DOI : 10.1103/PhysRevLett.84.951

[10] Z. Zheng, T. Wang, B. Jabar, D. Ao, F. Li, Y. Chen, G. Liang, J. Luo and P. Fan, Enhanced Thermoelectric Performance in n-Type Bi_2O_2Se by an Exquisite Grain Boundary Engineering Approach, ACS Appl. Energy Mater. 4 (2021) 10290-10297, DOI : 10.1021/acsaem.1c02219

[11] C. Tan, M. Tang, J. Wu, Y. Liu, T. Li, Y. Liang, B. Deng, Z. Tan, T. Tu, Y. Zhang, C. Liu, J. H. Chen, Y. Wang and H. Peng, Wafer-Scale Growth of Single-Crystal 2D Semiconductor on Perovskite Oxides for High-Performance Transistors, Nano Lett. 19 (2019) 2148-2153, DOI : 10.1021/acs.nanolett.9b00381

This preprint research paper has not been peer reviewed. Electronic copy available at: https://ssrn.com/abstract=4194617

[12] X. Zhang, Y. Liu, G. Zhang, Y. Wang, H. Zhang and F. Huang, Thermal Decomposition of Bismuth Oxysulfide from Photoelectric Bi_2O_2S to Superconducting $Bi_4O_4S_3$, ACS Appl. Mater. Interfaces, 7 (2015) 4442-4448, DOI : 10.1021/am5092159

[13] J. Wu, H. Yuan, M. Meng, C. Chen, Y. Sun, Z. Chen, W. Dang, C. Tan, Y. Liu, J. Yin, Y. Zhou, S. Huang, H. Q. Xu, Y. Cui, H. Y. Hwang, Z. Liu, Y. Chen, B. Yan and H. Peng, High electron mobility and quantum oscillations in non-encapsulated ultrathin semiconducting Bi_2O_2Se, Nat. Nanotechnol. 12 (2017) 530-534, DOI : 10.1038/nnano.2017.43

[14] J. Li, Z. Wang, Y. Wen, J. Chu, L. Yin, R. Cheng, L. Lei, P. He, C. Jiang, L. Feng and J. He, High-Performance Near-Infrared Photodetector Based on Ultrathin Bi_2O_2Se Nanosheets, Adv. Funct. Mater. 28 (2018) 1706437, DOI : 10.1002/adfm.201706437

[15] C. Chen, M. Wang, J. Wu, H. Fu, H. Yang, Z. Tian, T. Tu, H. Peng, Y. Sun, X. Xu, J. Jiang, N. B. M. Schröter, Y. Li, D. Pei, S. Liu, S. A. Ekahana, H. Yuan, J. Xue, G. Li, J. Jia, Z. Liu, B. Yan, H. Peng and Y. Chen, Electronic structures and unusually robust bandgap in an ultrahigh-mobility layered oxide semiconductor, Bi_2O_2Se, Sci. Adv. 4 (2018) eaat8355, DOI : 10.1126/sciadv.aat8355

[16] Z. Zhang, T. Li, Y. Wu, Y. Jia, C. Tan, X. Xu, G. Wang, J. Lv, W. Zhang, Y. He, J. Pei, C. Ma, G. Li, H. Xu, L. Shi, H. Peng and H. Li, Truly Concomitant and Independently Expressed Short- and Long-Term Plasticity in a Bi_2O_2Se-Based Three-Terminal Memristor, Adv. Mater. 31 (2019) 1805769, DOI : 10.1002/adma.201805769

[17] J. Yu and Q. Sun, Bi_2O_2Se nanosheet: An excellent high-temperature n-type thermoelectric material, Appl. Phys. Lett. 112 (2018) 053901, DOI : 10.1063/1.5017217

[18] J. Yang, R. Quhe, Q. Li, S. Liu, L. Xu, Y. Pan, H. Zhang, X. Zhang, J. Li, J. Yan, B. Shi, H. Pang, L. Xu, Z. Zhang, J. Lu and J. Yang, Sub 10 nm Bilayer Bi_2O_2Se Transistors, Adv. Electron. Mater. 5 (2019) 1800720, DOI : 10.1002/aelm.201800720

[19] X. Tan, Y. Liu, R. Liu, Z. Zhou, C. Liu, J. L. Lan, Q. Zhang, Y. H. Lin and C. W. Nan, Synergistical Enhancement of Thermoelectric Properties in n-Type Bi_2O_2Se by Carrier Engineering and Hierarchical Microstructure, Adv. Energy Mater. 9 (2019) 1900354, DOI : 10.1002/aenm.201900354

[20] P. Ruleova, C. Drasar, P. Lostak, C. P. Li, S. Ballikaya and C. Uher, Thermoelectric properties of Bi_2O_2Se, Materials Chemistry and Physics, 119 (2010) 299-302, DOI : 10.1016/j.matchemphys.2009.08.067

[21] C. Huang and H. Yu, Two-Dimensional Bi_2O_2Se with High Mobility for High-Performance Polymer Solar Cells, ACS Appl. Mater. Interfaces 12 (2020) 19643-19654, DOI : 10.1021/acsami.0c01364

[22] T. Yang, X. Li, L. Wang, Y. Liu, K. Chen, X. Yang, L. Liao, L. Dong and C.-X. Shan, Broadband photodetection of 2D Bi_2O_2Se–$MoSe_2$ heterostructure, J. Mater. Sci. 54 (2019) 14742-14751, DOI : 10.1007/s10853-019-03963-1

[23] T. Tong, Y. Chen, S. Qin, W. Li, J. Zhang, C. Zhu, C. Zhang, X. Yuan, X. Chen, Z. Nie, X. Wang, W. Hu, F. Wang, W. Liu, P. Wang, X. Wang, R. Zhang and Y. Xu, Sensitive and Ultrabroadband Phototransistor Based on Two-Dimensional Bi_2O_2Se Nanosheets, Adv. Funct. Mater. 29 (2019) 1905806-1905806, DOI : 10.1002/adfm.201905806

[24] X. Liu, R. Li, C. Hong, G. Huang, D. Pan, Z. Ni, Y. Huang, X. Ren, Y. Cheng and W. Huang, Highly efficient broadband photodetectors based on lithography-free Au/Bi_2O_2Se/Au heterostructures, Nanoscale 11 (2019) 20707-20714, DOI : 10.1039/C9NR06723J

[25] Y. Sun, S. Ye, J. Zhang, J. Song, F. Zhou and J. Qu, Lithium nitrate-assisted hydrothermal synthesis of ultrathin Bi_2O_2Se nanosheets and their photoelectrochemical performance, J. Mater. Chem. C 8 (2020) 14711-14717, DOI : 10.1039/D0TC04352D

This preprint research paper has not been peer reviewed. Electronic copy available at: https://ssrn.com/abstract=4194617

[26] L. Pan, L. Zhao, X. Zhang, C. Chen, P. Yao, C. Jiang, X. Shen, Y. Lyu, C. Lu, L. D. Zhao and Y. Wang, Significant Optimization of Electron–Phonon Transport of n-Type Bi_2O_2Se by Mechanical Manipulation of Se Vacancies via Shear Exfoliation, ACS Appl. Mater. Interfaces 11 (2019) 21603-21609, DOI : 10.1021/acsami.9b05470

[27] W. Kim, S. Arpiainen, H. Xue, M. Soikkeli, M. Qi, Z. Sun, H. Lipsanen, F. A. Chaves, D. Jimenez and M. Prunnila, Photoresponse of Graphene-Gated Graphene-GaSe Heterojunction Devices, ACS Appl. Nano Mater. 1 (2018) 3895-3902, DOI : 10.1021/acsanm.8b00684

[28] H. Qiao, J. Yuan, Z. Xu, C. Chen, S. Lin, YushengWang, J. Song, Y. Liu, Q. Khan, H. Y. Hoh, C.-X. Pan, S. Li and Q. Bao, Broadband Photodetectors Based on Graphene–Bi_2Te_3 Heterostructure, ACS Nano 9 (2015) 1886-1894, DOI : 10.1021/nn506920z

[29] A. K. Geim and I. V. Grigorieva, Van der Waals heterostructures, Nature 499 (2013) 419-425, DOI : 10.1038/nature12385

[30] E. Wu, D. Wu, C. Jia, Y. Wang, H. Yuan, L. Zeng, T. Xu, Z. Shi, Y. Tian and X. Li, In Situ Fabrication of 2D WS_2/Si Type-II Heterojunction for Self-Powered Broadband Photodetector with Response up to Mid-Infrared, ACS Photonics 6 (2019) 565-572, DOI : 10.1021/acsphotonics.8b01675

[31] K. Li, W. Wang, J. Li, W. Jiang, M. Feng and Y. He, High-responsivity, self-driven photodetectors based on monolayer WS_2/GaAs heterojunction, Photon. Res. 8 (2020) 1368-1374, DOI : 10.1364/PRJ.396880

[32] S. Shoaee, M. Stolterfoht and D. Neher, The Role of Mobility on Charge Generation, Recombination, and Extraction in Polymer-Based Solar Cells, Adv. Energy Mater. 8 (2018) 1703355, DOI : 10.1002/aenm.201703355

[33] P. Luo, F. Wang, J. Qu, K. Liu, X. Hu, K. Liu and T. Zhai, Self-Driven WSe_2/Bi_2O_2Se Van der Waals Heterostructure Photodetectors with High Light On/Off Ratio and Fast Response, Adv. Funct. Mater. 31 (2021) 2008351, DOI : 10.1002/adfm.202008351

[34] T. Yang, X. Li, L. Wang, Y. Liu, K. Chen, X. Yang, L. Liao, and C. Shan Broadband photodetection of 2D Bi_2O_2Se–$MoSe_2$ heterostructure, J. Mater. Sci. 54 (2019) 14742-14751, DOI : 10.1007/s10853-019-03963-1

[35] A. A. Khan, Z. Yu, U. Khan, and L. Dong, Solution Processed Trilayer Structure for High-Performance Perovskite Photodetector, Nanoscale Research Letters 13 (2018) 399, DOI : 10.1186/s11671-018-2808-7

[36] J. Ahn, J. H. Kang, M. C. Park and D. K. Hwang, All 2D WSe_2/MoS_2 heterojunction photodiode and its image sensor application, Opt. Lett. 45 (2020) 4531-4534, DOI : 10.1364/OL.399955

[37] B. Liu, B. Tang, F. Lv, Y. Zeng, J. Liao, S. Wang and Q. Chen, Photodetector based on heterostructure of two-dimensional WSe_2/In_2Se_3, Nanotechnology 31 (2020) 065203-065212, DOI : 10.1088/1361-6528/ab519b

[38] J. Sun, Q. Hua, R. Zhou, D. Li, W. Guo, X. Li, G. Hu, C. Shan, Q. Meng, L. Dong, C. Pan, and Z. L. Wang, Piezo-phototronic Effect Enhanced Efficient Flexible Perovskite Solar Cellsr, ACS Nano 13 (2019) 4507-4513, DOI : 10.1021/acsnano.9b00125

[39] X. Chen, X. Yang, Q. Lou, Y. Zhang, Y. Chen, Y. Lu, L. Dong, and C. Shan, Fabry-Perot interference and piezo-phototronic effect enhanced flexible MoS_2 photodetector, Nano Res. 15 (2022) 4395-4402, DOI : 10.1007/s12274-021-3989-4

[40] J. Tao, J. Chai, X. Lu, L. M. Wong, T. I. Wong, J. Pan, Q. Xiong, D. Chi and S. Wang, Growth of wafer-scale MoS_2 monolayer by magnetron sputtering, Nanoscale 7 (2015) 2497-2503, DOI : 10.1039/C4NR06411A

[41] Y. Liang, Y. Chen, Y. Sun, S. Xu, J. Wu, C. Tan, X. Xu, H. Yuan, L. Yang, Y. Chen, P. Gao, J. Guo and H. Peng, Molecular Beam Epitaxy and Electronic Structure of Atomically Thin Oxyselenide Films, Adv. Mater. 31 (2019) 1901964, DOI : 10.1002/adma.201901964

This preprint research paper has not been peer reviewed. Electronic copy available at: https://ssrn.com/abstract=4194617

[42] R. Kaindl, B. C. Bayer, R. Resel, T. Muller, V. Skakalova, G. Habler, R. Abart, A. S. Cherevan, D. Eder, M. Blatter, F. Fischer, J. C. Meyer, D. K. Polyushkin and W. Waldhauser, Growth, structure and stability of sputter-deposited MoS_2 thin films, Beilstein J. Nanotechnol 8 (2017) 1115-1126, DOI : 10.3762/bjnano.8.113

[43] U. P. Rathod, B. Cai, C. Iheomamere, G. Nyandoto, A. A. Voevodin and N. D. Shepherd, Growth of pulsed laser deposited few-layer WS_2 films, Journal of Vacuum Science & Technology A 37 (2019) 051505, DOI : 10.1116/1.5111727

[44] S. C. Xu, B. Y. Man, S. Z. Jiang, A. H. Liu, G. D. Hu, C. S. Chen, M. Liu, C. Yang, D. J. Feng and C. Zhang, Direct synthesis of graphene on any nonmetallic substrate based on KrF laser ablation of ordered pyrolytic graphite, Laser Phys. Lett. 11 (2014) 096001, DOI : 10.1088/1612-2011/11/9/096001

[45] G. Siegel, Y. P. Venkata Subbaiah, M. C. Prestgard and A. Tiwari, Growth of centimeter-scale atomically thin MoS_2 films by pulsed laser deposition, APL Mater. 3 (2015) 056103, DOI : 10.1063/1.4921580

[46] S. Seo, S. Kim, H. Choi, J. Lee, H. Yoon, G. Piao, J. C. Park, Y. Jung, J. Song, S. Y. Jeong, H. Park and S. Lee, Direct In Situ Growth of Centimeter-Scale Multi-Heterojunction MoS_2/WS_2/WSe_2 Thin-Film Catalyst for Photo-Electrochemical Hydrogen Evolution, Adv. Sci. 6 (2019) 1900301, DOI : 10.1002/advs.201900301

[47] S. Seo, I. Oh, J.-C. Park, J. Lee, Y. Jung, H. Choi, J. Ryu and S. Lee, Growth of Transition Metal Dichalcogenide Heterojunctions with Metal Oxides for Metal–Insulator–Semiconductor Capacitors, ACS Appl. Nano Mater. 4 (2021) 12017-12023, DOI : 10.1021/acsanm.1c02547

[48] J. Yin, Z. Tan, H. Hong, J. Wu, H. Yuan, Y. Liu, C. Chen, C. Tan, F. Yao, T. Li, Y. Chen, Z. Liu, K. Liu and H. Peng, Ultrafast and highly sensitive infrared photodetectors based on two-dimensional oxyselenide crystals Nat. Commun. 9 (2018) 3311, DOI : 10.1038/s41467-018-05874-2

[49] Z. Liu, C. Wang, Z. Zhu, Q. Lou, C. Shen, Y. Chen, J. Sun, Y. Ye, J. Zang, L. Dong, and C. Shan, Wafer-scale growth of two-dimensional graphitic carbon nitride films, Matter 4 (2021) 1625-1638, DOI : 10.1016/j.matt.2021.02.014

[50] A. J. Khadpekar, M. Khan, A. Sose and A. Majumder, Low Cost and Lithography-free Stamp fabrication for Microcontact Printing, Sci. Rep. 9 (2019) 1024, DOI : 10.1038/s41598-018-36521-x

[51] T. V. Hakkarainen, A. Schramm, J. Makela, P. Laukkanen and M. Guina, Lithography-free oxide patterns as templates for self-catalyzed growth of highly uniform GaAs nanowires on Si(111), Nanotechnology 26 (2015) 275301, DOI: 10.1088/0957-4484/26/27/275301

[52] X. Chen, Y. J. Park, T. Das, H. Jang, J. B. Lee and J. H. Ahn, Lithography-free plasma-induced patterned growth of MoS_2 and its heterojunction with graphene, Nanoscale 8 (2016) 15181-15188, DOI: 10.1039/C6NR03318K

[53] A. Kim, K. S. Jang, J. Kim, J. C. Won, M. H. Yi, H. Kim, D. K. Yoon, T. J. Shin, M. H. Lee, J. W. Ka and Y. H. Kim, Solvent-Free Directed Patterning of a Highly Ordered Liquid Crystalline Organic Semiconductor via Template-Assisted Self-Assembly for Organic Transistors, Adv. Mater. 25 (2013) 6219-6225, DOI: 10.1002/adma.201302719

[54] A. Mohammed, H. Nakamura, P. Wochner, S. Ibrahimkutty, A. Schulz, Pulsed laser deposition for the synthesis of monolayer WSe_2, Appl. Phys. Lett. 111 (2017) 073101, DOI: 10.1063/1.4986851

[55] T. Cheng, C. Tan, S. Zhang, T. Tu, H. Peng and Z. Liu, Raman Spectra and Strain Effects in Bismuth Oxychalcogenides, J. Phys. Chem. C 122 (2018) 19970-19980, DOI:10.1021/ACS.JPCC.8b05475

[56] Y. Guo, Y. Song, M. Yang, Z. Xu, H. Xie, H. Li, Z. Li, H. Liang, S. Ruan and Y.-J. Zeng,Unveiling interface interaction assisted broadband photoresponse of epitaxial 2D Bi_2O_2Se on perovskite oxides, J. Mater. Chem. C 8 (2020) 13226-13234, DOI: 10.1039/D0TC03245J

This preprint research paper has not been peer reviewed. Electronic copy available at: https://ssrn.com/abstract=4194617

[57] M. Varshney, Y. Li, B. Srinivasan and S. Tung, A label-free, microfluidics and interdigitated array microelectrode-based impedance biosensor in combination with nanoparticles immunoseparation for detection of Escherichia coli O157:H7 in food samples, Sens. Actuators B: Chem. 128 (2007) 99-107, DOI: 10.1016/j.snb.2007.03.045

Preprint not peer reviewed

This preprint research paper has not been peer reviewed. Electronic copy available at: https://ssrn.com/abstract=4194617

Entry for the Table of Contents

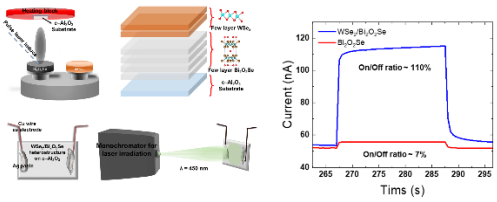

A simple device fabrication process using pulsed laser deposition is proposed to fabricate the heterostructure of WSe_2/Bi_2O_2Se thin films. The developed device has a high photodetection performance with a 110% on/off ratio without a lithography process for interdigitated electrode patterns.

Preprint not peer reviewed

This preprint research paper has not been peer reviewed. Electronic copy available at: https://ssrn.com/abstract=4194617